Article

Not peer-reviewed version

Expression of Syntaxin 18 in *Peregrinus maidis* and Design of Its dsRNA Fragments towards a Targeted RNAi Biopesticide for Insect Vector Control

Hannah Corinne T. Cantaros , Charlene Niebres , Ruth Alessandra Banasihan , Argel L. Arenas , Karen B. Alviar *

Posted Date: 20 September 2024

doi: 10.20944/preprints202409.1580.v1

Keywords: Corn planthopper; Maize mosaic virus; RNAi; Syntaxin 18

Article

Expression of Syntaxin 18 in *Peregrinus maidis* and Design of Its dsRNA Fragments towards a Targeted RNAi Biopesticide for Insect Vector Control

Running title: PmStx18 expression and dsRNA design

Hannah Corinne T. Cantaros [1], Charlene Niebres [2,3], Ruth Alessandra Banasihan [3], Argel L. Arenas [1] and Karen B. Alviar [3,*]

[1] Institute of Biological Sciences, Cell and Molecular Biology Division, University of the Philippines, Los Baños, Philippines
[2] DOST- Philippine Textile Research Institute, Bicutan, Taguig City, Philippines
[3] Institute of Weed Science Entomology and Plant Pathology, College of Agriculture and Food Science, University of the Philippines, Los Baños, Philippines
* Correspondence: and first author: kbalviar@up.edu.ph

Abstract: Maize mosaic virus (MMV) is a plant virus that is transmitted by the corn planthopper, *Peregrinus maidis* Ashmead (Hemiptera: Delphacidae) in a persistent and propagative manner. MMV is the causal agent for mosaic disease that can cause significant loss in corn yield. Management is focused on controlling insect vector population. The molecular mechanisms of virus transmission by the insect vector are not fully understood. Previously, we identified a receptor for MMV, the *P. maidis* syntaxin 18 (PmStx18). PmStx18 interacts with the viral glycoprotein and potentially facilitates MMV recognition and entry into the vector, enabling virus proliferation. Stx18 is a key component of the vesicular trafficking machinery and also plays a critical role in neurotransmitter release in insects. In this work, we investigated the expression of PmStx18 in different developmental stages and major parts of the insect vector. Primers were designed to generate templates for synthesis of double-stranded RNA fragments. A 374-bp amplicon was selected and gene-specific sequences were flanked by T7 promoter sequences for in vitro transcription. Results showed a significant difference in the expression of Stx18 in the different developmental stages of *P. maidis* but not between male and female adults and major body parts. In vitro transcription products indicated optimal reaction conditions and protocol suitability. The findings establish the initial steps for developing RNAi-based approach in controlling MMV transmission by targeting Syntaxin-18 in *P. maidis*. Further investigations are needed to evaluate the efficacy of this approach.

Keywords: Corn planthopper; Maize mosaic virus; RNAi; Syntaxin 18

Introduction

Maize mosaic virus (MMV) is a plant virus that is transmitted by the corn planthopper, *Peregrinus maidis* in a persistent and propagative manner. MMV is a progressive neurotropic virus of the family Rhabdoviridae, genus alphanucleorhabdoviridae. To date, around 160 species of rhabdoviruses have been documented, infecting a wide range of hosts that include humans and vertebrates, invertebrates, and plants. At least 90 of these are plant-pathogenic viruses. Some important rhabdoviruses are the Rabies virus (RV), which accounts for an estimated 59,000 human deaths in over 150 countries annually, and Vesicular stomatitis virus (VSV), which infects horses and cattle. When it comes to plant rhabdoviruses, notable ones such as the Maize mosaic virus (MMV), Lettuce necrotic yellows virus (LNYV), Strawberry crinkle virus (SCV) and Orchid fleck virus (OFV) have been known to cause yield losses (Ammar et al., 2009). MMV shares with other rhabdoviruses the appearance of a distinct, bullet-shaped, bacilliform virion possessing a host-derived lipid

 doi:10.20944/preprints202409.1580.v

envelope. It is a negative-sense, single-stranded RNA virus whose genome is 12,133 bp long, consisting of five/six protein-coding genes in the antigenomic order 5′-N-P-3-M-G-L-3′ (Reed et al., 2005). The nucleoprotein (N) is an icosahedral capsid that encapsidates the viral genomic RNA and is part of the viroplasm and polymerase complex. The phosphoprotein (P) is a polymerase cofactor, interacting with N and L during replication, mediating N and L intracellular movement, and functions in gene suppression and silencing. 3 is a putative cell-to-cell movement protein. M is a matrix protein, mediating membrane-lipid interactions with the G protein and is involved in regulation of host gene expression and has been shown to interact with mitochondria. G forms the surface glycoprotein that is involved in viral entry into host cells, which is achieved through G and receptor binding followed by membrane fusion. L encodes an RNA-dependent polymerase protein. In the case of MMV, L is responsible for mRNA transcription and antigenomic and genomic RNA replication (Ammar et al., 2009).

The corn planthopper *P. maidis* belongs to the order Hemiptera, and the suborder Auchenorrhyncha, a group of sap-sucking insects that also consist of cicadas, spittlebugs, leafhoppers, treehoppers, and other planthoppers (Dietrich, 2009). The corn planthopper is a tropical phytophagous insect that is widely distributed across the globe. On average, the insect can complete its life cycle within a month in tropical countries such as the Philippines but can reach over 75 days in temperate regions. Adults and nymphs of *P. maidis* colonize the leaf whorls and sheaths. Corn planthopper feeding commences by injecting watery saliva that aids in digestion into the plant and ingesting the fluid from the plant phloem (Dietrich, 2009). The feeding and removal of sap from leaves account for most of the damage caused by the corn planthopper since it disrupts the photosynthetic flow, mobility of nutrients, and sink-source relationships of infested plants. It also predisposes its plant hosts to moisture stress and sooty mold development. Direct damage may also be caused by oviposition of female *P. maidis* on the midrib of leaves, which causes reddening and desiccation of the plant tissue around the eggs (Balikai et al., 2017). It is important to note that *P. maidis* acquires and transmits MMV and Maize strip virus (MStpV) to plants through this manner of plant sap feeding. MMV is transmitted by *P. maidis* in a persistent and propagative manner. For this to occur, *P. maidis* nymphs and adults acquire MMV through feeding of sap from infected plants and transmit it to healthy ones (Barandoc-Alviar et al., 2016). Immunofluorescence confocal laser scanning microscopy of MMV-infected planthoppers revealed a neurotropic dissemination route of the virus within its insect vector (Ammar and Hoggenhout, 2008). The virus from the infected plant sap has to travel through the esophagus, into the midgut, where MMV has been shown to initially accumulate, specifically within the epithelial cells of the anterior part of the insect midgut and anterior diverticulum. MMV infection then progresses into the nerve cord and compound ganglionic mass at least a week before the virus systemically spreads to other tissues such as hemocytes, tracheae, and salivary glands. Invasion of MMV into *P. maidis* salivary glands ultimately allows the virus to be transmitted to healthy plants when the insect feeds (Jackson et al., 2008, Ammar and Hogenhout, 2008). This progression pattern of MMV within *P. maidis* suggests two things: i) there exists midgut exit barriers and salivary gland infection barriers and ii) MMV uses a neurotropic route to overcome these barriers. Although the hemolymph route is also viable for MMV, a neurotropic route is consistent with the mechanisms of other rhabdoviruses, such as Rabies virus, which reaches the salivary glands of its infected hosts and vectors through invasion of the nervous system. An analysis of acquisition and virus titer over time across developmental stages of *P. maidis* has shown that planthopper nymphs are more efficient in acquiring MMV than adults. In addition, virus titer was shown to continuously increase as the planthopper nymphs developed into adults. The same study found that virus titer also differed significantly in males and females, with males having a mean viral titer that is fourfold higher than females (Barandoc-Alviar et al., 2016).

MMV and other plant rhabdoviruses have evolved several mechanisms to circumvent the barriers to infection present in their insect and plant hosts. MMV displays broad tissue tropism in the insect body despite various infection barriers. It is postulated that MMV acquisition by *P. maidis* involves virus attachment to specific receptors in the midgut, followed by active translocation to other insect tissues. Interacting proteins in the insect host with MMV that support its infection and

 doi:10.20944/preprints202409.1580.v

replication have been identified both in silico and *in vivo*. Using membrane-based yeast two-hybrid (MbY2H) assay, Barandoc-Alviar et al. (2022) identified 125 proteins in *P. maidis* that physically interacted with MMV G protein. Majority (68%) of these proteins are associated with a diverse array of functions such as endocytosis, vesicle-mediated transport, protein synthesis and turnover, nuclear import and export, metabolism, and host defense. MbY2H identified Apolipophorin III (ApoLpIII) and Cyclophilin A (CypA) as interacting proteins and were also found to co-localize with MMV-G in a heterologous insect cell system. Cyclophilins are peptidyl-prolyl *cis-trans*-isomerases that are involved in protein folding and trafficking, cell signaling, immune responses and interactions between plant viruses and their insect and plant hosts. CypA in particular has been shown to be central to the replication or transport of viruses such as HIV-1, Tomato spotted wilt virus (TSWV), and VSV-NJ. ApoLpIII is an insect apolipoprotein that functions in lipid transport, pathogen pattern recognition, and multicellular encapsulation reactions as a component of the innate immune response. ApoLpIII, being abundant in the insect hemolymph, hemocytes, eggs, and fat body, is positioned as a possible receptor of MMV in its hemocyte route of infection. Interactions of MMV-G with ApoLpIII and Cyp A were further confirmed through co-immunoprecipitation assays. MbY2H also revealed MMV-G interactions with Syntaxin 18, small GTPase Rab2, nucleoside diphosphate kinase (NDK), and E3 ubiquitin protein ligase MARCH3 (Membrane-associated RING-CH), all of which are proteins involved in clathrin-dependent receptor-mediated endocytosis (Barandoc- Alviar et al., 2022). Syntaxin 18 in particular, is positioned as a putative receptor of MMV in its neural route of infection.

Syntaxin 18 is from the soluble NSF-attachment protein receptor (SNARE) protein family. SNARE proteins exhibit significant roles in neurotransmitter release and many other forms of membrane fusion. These proteins are like molecular motors that drive the biological fusion of two membranes enabling the transport and delivery of cargo within the cell (Liu et al., 2023). In insects, SNARE proteins have been implicated in a wide range of physiological functions such as secretion of hormones, release of neurotransmitters, and membrane trafficking (He et al., 2018). Syntaxins are broadly expressed. Syntaxin 1A and Syntaxin 1B are localized in the presynaptic plasma membrane in neuronal and secretory cells of the brain. They have been found to mediate neuronal exocytosis and neurotransmitter release. Recently, Syntaxin 1 along with Syntaxins 5 and 15 were found to play a crucial role in the growth and maintenance of seamless tubes in the trachea of *Drosphila. melanogaster* (Bourne et al., 2021). Syntaxin 2 is ubiquitously expressed and is localized to the plasma membrane. Syntaxin 2 acts as a morphoregulator during development and also functions in exocytosis. Syntaxins 15, 3, and 4 are localized in the plasma membrane of cells of the heart, spleen, lung and kidney, and are involved in exocytosis and Glut4 translocation, respectively. Syntaxin 6 and 16 are localized to the *trans*-Golgi Network (TGN) and function in TGN-endosome transport. Syntaxin 10 is also localized in the TGN, but its functions have not yet been defined. Syntaxins 7, 8, 12 and 13 are localized in endosomes. Syntaxin 7 and 8 function in late endosome fusion, while Syntaxins 12 and 13 are involved in the recycling of surface protein and early endosome fusion (Teng et al., 2001). Syntaxin 11 is localized in endosomes of immune cells and has been found to regulate lipid metabolism and lipophagy in hepatocytes by binding to adipose triglyceride lipase (ATGL) and preventing lipid droplet destruction and autophagy (Zhang et al., 2022). Syntaxin 17 is localized in the smooth endoplasmic reticulum (ER) of steroidogenic tissues and functions in trafficking to the smooth ER. Syntaxin 17 is a Qa SNARE that recruits Snap29 to mature autophagosomes to facilitate fusion with lysosomes, exposing the V-SNARE VAMP8 (Smeele and Vaccari, 2022). Syntaxin 18 is a more novel member of the SNARE protein family, whose functions have yet to be fully characterized. According to Hatsuzawa et al. (2000), Syntaxin 18 is a t-SNARE protein that functions in the ER, intermediate compartment, and cis-Golgi vesicle trafficking. Overexpression of Syntaxin 18 and a mutant version lacking its N-terminal domain has confirmed that it specifically interacts with and affects the structure of organelles involved in the early secretory pathway. *P. maidis* Syntaxin 18 has been shown to interact with MMV G, and its interactions and involvement in the docking of the virus have been demonstrated in silico (Alviar et al., 2022; Castrosanto et al., 2022). Syntaxin 18 in *D. melanogaster* has sometimes been referred to as guanylate kinase-like (GUK)-interacting syntaxin or

 doi:10.20944/preprints202409.1580.v

Gtaxin (GTX). In *D. melanogaster*, Syntaxin 18 was reportedly isolated from neuromuscular cells as a DLG-interacting (Drosophila Discs-Large) SNARE protein that mediates DLG-dependent addition of postsynaptic membranes during synapse development via vesicle fusion (Gorczyca et al., 2007). GTX shares similarity of sequence with vertebrate Syntaxin-18 (Hatsuzawa et al., 2000) and Ufe1p from yeast (Lewis et al., 1997). Ufe1p was found to mediate homotypic endoplasmic reticulum membrane fusion in the absence of any other known SNARE (Patel et al., 1998).

The molecular mechanisms of virus transmission by insect vectors transmitting persistent propagative plant viruses are not fully understood. The *P. maidis* and MMV pathosystem, is a model system, which has been used to elucidate the complex mechanism involved in the acquisition, replication and transmission of viral phytopathogens. In this work, we investigated the expression of *P. maidis* syntaxin 18 (PmStx18), in different developmental stages of the insect vector and its three main parts, the head, thorax and abdomen. An analysis of Syntaxin 18 expression should shed light on virus-vector interactions, and comparing expression in *P. maidis* developmental stages, sex and wing type may reveal important host factors that modulate virus infection. We synthesized double-stranded RNA targeting fragments of Stx18. Our study provides new insights into the insect vector's syntaxin expression and highlights the potential of targeting it as a novel strategy for controlling MMV through innovative plant protection strategy such as RNA interference.

Materials and Methods

Insect Rearing and Sampling

Corn planthoppers (*Peregrinus maidis*) were originally collected from the Central Experiment Station in Pili Drive, UPLB in 2019. They were maintained in 30 cm x 30 cm x 60 cm cages covered by nylon-mesh screen in a screen house. Corn seeds (Lagkitan) were obtained from the Institute of Plant Breeding in Laguna, Philippines. Corn plants were grown on garden soil supplemented with complete fertilizer and Urea following agronomic practices. Two rearing cages containing four pots of corn, with four corn plants in each pot, were prepared. Corn plants were watered everyday throughout the length of the study. Cages were also monitored every day for the presence of any other insect or predator that could compromise the rearing of *P. maidis*. Three weeks after planting, 50 pairs of *P. maidis* adults were introduced to each rearing cage. The planthoppers were allowed to oviposit for one week and the eggs were allowed an incubation period of another week. The corn plants were replaced every two weeks. Stratified random sampling was performed to select specimens from nymphal stages I to IV, and macropterous and brachypterous adults. Per replicate, 30 planthoppers were collected for the first and second instars, 20 planthoppers for the third instar, 10 planthoppers for the fourth instar, and five planthoppers for each sex and each wing type in the adult stage. Sex determination was done by checking for the absence or presence of ovipositors. Samples were collected in 1.5-mL microcentrifuge tubes and stored in -20ºC prior to RNA extraction.

Total RNA Extraction and cDNA Synthesis

Total RNA was isolated from the eight groups corresponding to the life stages *of P. maidis* samples using ReliaPrep™ RNA Miniprep (Promega, Fitchburg, WI, USA), following the protocol for extraction from fibrous animal tissue. Prior to extraction, LBA + TG buffer, RNA wash solution, and column wash solution were prepared. Samples were homogenized in 500 µL LBA+TG buffer with the aid of a micropestle. RNA dilution buffer (500 µL) was added to the lysis mixture and was incubated for one minute at room temperature before centrifuging for 3 minutes at 10,000 x g to pellet cellular debris. The lysates were transferred to clean microcentrifuge tubes. Isopropanol (340 µL) was added to the lysates and was flicked gently to mix. The lysates were transferred to minicolumns and placed in collection tubes and centrifuged for 1 minute at 14,000 x g. This was performed twice, with 670 µL of lysate being processed at a time. The liquid in the collection tube was discarded and 500 µL of RNA wash solution was added to the minicolumn. This was centrifuged at 14,000 x g for 30 seconds. DNase I incubation mix that consisted of 24 µL yellow core buffer, 3 µL $MnCl_2$, and 3 µL DNase I enzyme per sample was prepared. The 30 µL DNase I mix was pipetted directly onto the

 doi:10.20944/preprints202409.1580.v

membrane of each minicolumn. After 15 minutes of incubation at room temperature, 200 µL of column wash solution was added to each minicolumn and centrifuged at 14,000 x g for 15 seconds. RNA wash solution (500 µL) was added and centrifuged for 30 seconds at 14,000 x g. Another round of RNA wash was performed, adding 300 µL of RNA wash solution and centrifuging for 2 minutes at 14,000 x g. The RNA was eluted using 20ul nuclease-free water into 1.5-mL elution tubes. All RNA extracts were stored in -20ºC at all times. The concentration of the RNA isolates were measured by microvolume UV spectrophotometry using Epoch microplate spectrophotometer (Agilent Biotek, Winooski, VT, USA) at 260nm absorbance. The quality of RNA isolates were measured at A_{260}/A_{280}. Only A_{260}/A_{280} ratios of 1.8-2.1 were used for further analysis.

First strand cDNA synthesis was performed on 1 µg of total RNA using Viva cDNA synthesis kit (Vivantis, Selangor, Malaysia) following the protocol advised by the manufacturer, with a modification of using a mixture of 1 µL of Oligo d(T) and 1 µL of random hexamers as primers. The use of both Oligo d(T) and random hexamers as primers aims to give a higher yield of cDNA. The RNA-primer mixture was incubated at 65ºC for five minutes and then chilled on ice for two minutes afterwards. The prepared cDNA synthesis mixture (10 µL) was transferred to each of the RNA-primer mixtures and centrifuged briefly. After centrifugation, the mixture was incubated for one hour at 42ºC to allow the reverse transcription to occur. To terminate the reaction, the tubes were incubated at 85ºC for five minutes, and were then transferred to ice and centrifuged briefly. All synthesized cDNA were stored at -20ºC.

Primer Design

Primers specific to PmStx18 for semi-quantitative PCR were designed using the NCBI-Primer Blast tool. Primer sequences were based on the PmStx18 sequence from the yeast two hybrid screening of Alviar et al. (2022). This sequence was aligned using BLASTn with parameters set to search for highly similar sequences (megablast). The brown planthopper *Nilaparvata lugens* predicted Syntaxin 18 mRNA sequence (NCBI Accession: XM_022335761) that matched with 88.66% identity and e-value of $5e^{-109}$ was aligned with PmStx18 using EMBL-EBI Multiple Sequence Alignment Tool ClustalW. Degenerate primers were designed manually based on the generated consensus sequence. Primers were designed based on the following parameters: sequence length between 18-25 bases, Tm difference of not more than 5ºC, presence of one GC clamp, GC content of 40-65%, and amplicon length of at least 500 bp. Primer sequences were screened for possible formation hairpins and for the presence of single and double nucleotide base runs using the Sequence Manipulation Suite: PCR Primer Stats (Stothard, 2000). Only sequences that passed all tests were used as primers. *P. maidis* β-tubulin was used as an internal reference gene, using primer sequences previously designed and used by Barandoc-Alviar et al. (2016). A total of five primers were designed to target PmStx18, each targeting a different region of the mRNA sequence.

Dissection of P. maidis into Three Main Parts

Adult insects were dissected into their three main parts: head, thorax, and abdomen, using sharpened entomology pins with a 0.25 mm thickness and forceps. Sharpening stones is necessary to ensure precision in dissection. A stereomicroscope with a magnification between X10 and X30 was used to further improve the accuracy of dissection (Piou et al., 2021). Before dissection, the collected parts were initially weighed. The insect samples were then prepared, sprayed with 75% ethanol and air-dried for 3 minutes. The dried sample was then dissected using sharpened entomology pins with 0.25 mm thickness and forceps on 75% ethanol on a clean petri dish and collected in a microtube by their parts. The parts were then kept at -20ºC for storage or immediately subjected to RNA extraction.

PCR Optimization

All PCR amplification performed in this study used the Vivantis PCR kit 1 (Vivantis, Selangor, Malaysia). Optimization was performed on two sets of samples, consisting of pools of five adult planthoppers, five 4th instar nymphs, and a pool of five planthoppers each of nymphal stages I to III

 doi:10.20944/preprints202409.1580.v

to represent early nymphs. All five primers targeting PmStx18 were evaluated and optimal annealing temperatures for each were determined through gradient PCR with a thermal gradient of 48-55ºC for primer pairs F1R1 and F2R2 and a gradient of 50-55ªC for primer pairs F3R3, F4R4, F5R5. The amount of other PCR reagents and PCR parameters followed the recommended protocol of the kit manufacturer. The PCR program started with initial denaturation at 94ºC for 2 minutes, followed by 30 cycles of denaturation at 94ºC for 2 seconds, annealing for 30 seconds, extension at 72ºC for 30 seconds, and a final extension at 72ºC for 7 minutes. After gradient PCR, the samples were electrophoresed on 1.5% agarose gel at 80 V running for 1 hour. The gels were stained in GelRed in 1X TAE buffer for 30 minutes before digital capturing using BioBase gel documentation system (BioBase, Shandong, China). Primers that were able to yield amplicons of the correct target size were selected for quantitative endpoint PCR and the annealing temperature for each primer that resulted in the highest band intensity without the presence of nonspecific PCR products were adopted.

Endpoint Quantitative Reverse Transcription-Polymerase Chain Reaction (RT-PCR)

Endpoint quantitative RT- PCR was performed to measure gene expression of PmStx18. The quantity of amplified target is directly proportional to the input amount of target only during the linear range of amplification, i.e., at a fixed cycle set for the reaction (Schmittgen et al., 2000). All cDNA samples were diluted twice before undergoing PCR. For amplification of PmSTX18, the degenerate primer pair PmStx18-F5R5 with forward sequence 5′- CGATACTGGTGCKCAAAGGAT-3′ and reverse sequence 5′- CTTAGRCTRGCACTGCTTTCAA-3′ was used. The PCR master mix used followed the recommended volumes indicated in the Vivantis PCR kit 1. Initial denaturation was set at 94ºC for 2 minutes, followed by 30 cycles of denaturation at 94ºC for 2 seconds, annealing for 30 seconds, extension at 72ºC for 30 seconds, and a final extension set at 72ºC for 7 minutes. The annealing temperatures used for primers PmSTX18F5R5, PmSTX18F3R3, and BTUB were 55ºC, 54ºC, and 55ºC, respectively. Quantitation used β-tubulin as a reference gene, based on the assumption that this housekeeping gene is consistently expressed at similar levels across all samples. Amplicons (5 µL with 0.8 µL loading dye) were electrophoresed on 1.5% agarose gel at 80 V running for 1 hour. The gels were stained in GelRed in 1X TAE buffer for 30 minutes before digital capturing using the BioBase gel documentation system. Quantitation was done using Gel Pro Analyzer, wherein band intensity was expressed as relative absorbance units. PmStx18 expression was measured relative to β-tubulin expression.

PCR Product Purification and Sequencing

After confirmation of DNA band on gel electrophoresis, the PCR product was purified using GF-1 PCR Clean up kit (Vivantis, Selangor, Malaysia). Pools of four 50µL PCR products each from fourth nymphal stage and female macropters were chosen for purification due to their high band intensities. Buffer PCR (1 ml) was added to each pool of sample and vortexed for 10 seconds. The samples were loaded twice into a column in clean collection tubes and centrifuged for 1 minute at 10,000 x g. The column was washed with 750 µL of wash buffer and centrifuged at 10,000 x g for 1 minute. The column was dried of residual ethanol by centrifuging at 10,000 x g for another minute. The purified DNA was eluted into labeled 1.5-mL centrifuged tubes using 35uL of elution buffer. The purified DNA along with 10uM solutions of primers PmStx18-F5 and PmStx18-R5 were sent to Noveaulab Asia Corporation for single-pass Sanger sequencing.

Contig sequence was obtained from the sequencing results using Cap3 Contig Assembly. Contig sequence was aligned with the original PmStx18 mRNA sequence to verify the identity of isolated DNA using ClustalW.

Primer Design for In-Vitro Synthesis of dsRNA Fragments for RNAi

SnapDragon which is a web-based tool for designing double-stranded RNAs (dsRNAs) was employed to generate primers targeting PmStx18 gene. The PmStx18 mRNA sequence (Accession Number: OQ645740.1) was retrieved from NCBI and submitted to SnapDragon for primer design

 doi:10.20944/preprints202409.1580.v

where the desired dsRNA fragment length was set between a minimum of 200 base pairs to a maximum of 500 base pairs. Three primer pairs were selected based on having the same reverse primer sequence and low pair penalty to ensure their suitability for PCR amplification under standard conditions. A new set of primers was designed based on the previously selected gene-specific primers for dsRNA where extended T7 RNA polymerase promoter sequences (5′GGATCCTAATACGACTCACTATAGG3′) are attached to the 5′ end of the primers to improve efficiency of transcription. The few extra bases upstream of the minimal T7 promoter sequence enhances polymerase binding. The additional sequence can also function as a restriction enzyme cut site for future applications. Subsequently, the selected primer pairs were ordered from Kinovett Scientific Solution Co., Quezon City, Philippines.

Generation of DNA Templates with T7 Promoter Sequences

Two separate PCR amplification were performed to generate DNA templates containing T7 RNA polymerase promoters for in vitro transcription. Primers containing the T7 promoter sequence at the 5′ end were used in these reactions. Thermal cycling conditions were formulated based on the manufacturer's protocol for the T7 RiboMAX™ Express RNAi System (Promega, Fitchburg, USA). The initial PCR cycling conditions included 5-10 cycles at an annealing temperature 5°C higher than the melting temperature of the gene-specific sequences. This was followed by another three-step amplification with 20-35 cycles for each step. The annealing temperature for the subsequent cycles was 5°C higher than the melting temperature of the entire primer including the T7 promoter sequence. The duration per cycle was adapted from optimization strategies by Lorenz (2012). The specific thermal cycling parameters used are shown in Table 1. The resulting PCR products were analyzed by agarose gel electrophoresis to confirm amplification of a single band with the expected size.

Table 1. Thermal cycling parameters for the generation of DNA templates containing T7 RNA polymerase promoters.

	PCR STEP	TEMPERATURE (in °C)	DURATION (in sec)
Stage 1	Initial Denaturation	94	60
Stage 2 (5 Cycles)	Denaturation	94	20
	Annealing	63	30
	Extension	72	60
Stage 3 (30 Cycles)	Denaturation	94	60
	Annealing	75	30
	Extension	72	30
Stage 4	Final Extension	72	180
	Hold	4	

Statistical Analysis

Statistical analyses were performed on Jamovi (version 2.2.4) and Statistical for Agricultural Research (STAR- 2.0.1). The Shapiro–Wilk test was used to evaluate normality of data gathered, while Levene's homogeneity test was performed on relative PmStx18 expression values and BTub expression values. Quantities of PmStx18 and B-tubulin must not vary significantly within the same type of sample. In determining the significance of PmStx18 differential gene expression across different developmental stages, the mean calibrated values were analyzed using one-way ANOVA. For evaluation of significance of means among samples, results undergone Games-Howell post-hoc test. All statistical tests were done at 5% level of significance.

 doi:10.20944/preprints202409.1580.v

Results and Discussion

In this study, we conducted spatiotemporal analysis of Syntaxin 18 expression in *P.maidis.* PmStx18 was isolated and its expression was estimated across its developmental stages and in specific tissues. PmStx18 is found to be expressed across all developmental stages. Figure 1 shows PmStx18 expression based on the ratio of Absorbance values of Stx18 and B-tubulin. Our working assumption in this study is that all corn planthoppers that underwent analyses were not infected with MMV. The results of high PmStx18 expression in first and fourth instar nymphs are consistent with the findings of studies on acquisition efficiency of MMV in *P. maidis* first instar nymphs versus adults that have conclusively shown that nymphs acquire MMV significantly more efficiently than adults do. PmStx18 expression being highest in the first and fourth nymphal stages may allow *P. maidis* adults to support higher titers of MMV when acquired at the nymphal stage. Our results show that PmStx18 expression in adults is lower than in first and fourth instars, but the differences are not statistically significant. Our results also indicate that PmStx18 expression is higher in females than in males, and although it is not statistically significant, it is contrary to the observation that male brachypters support higher MMV titer by up to four-fold higher than females. Endpoint quantitative RT-PCR is not sensitive enough to measure small changes in transcript level. It is intriguing that PmStx18 expression dips in the second and third nymphal stages, only to increase in expression in the fourth nymphal stage. Analyses of temporal MMV titer reported that MMV titer in nymphal stages were not significantly different from each other and that the increase in titer was gradual but were significantly different from MMV titer in adults (Barandoc-Alviar et al., 2015), (Barandoc-Alviar et al., 2016). Low expression of the putative receptor of MMV in second and third nymphal stages could explain the statistically insignificant rise in MMV titer amongst instars. It is unlikely that the low PmStx18 expression detected in second and third instars was due to experimental error or contamination since the concentration of total RNA across all samples were normalized and the purity of all samples were within the recommended range.

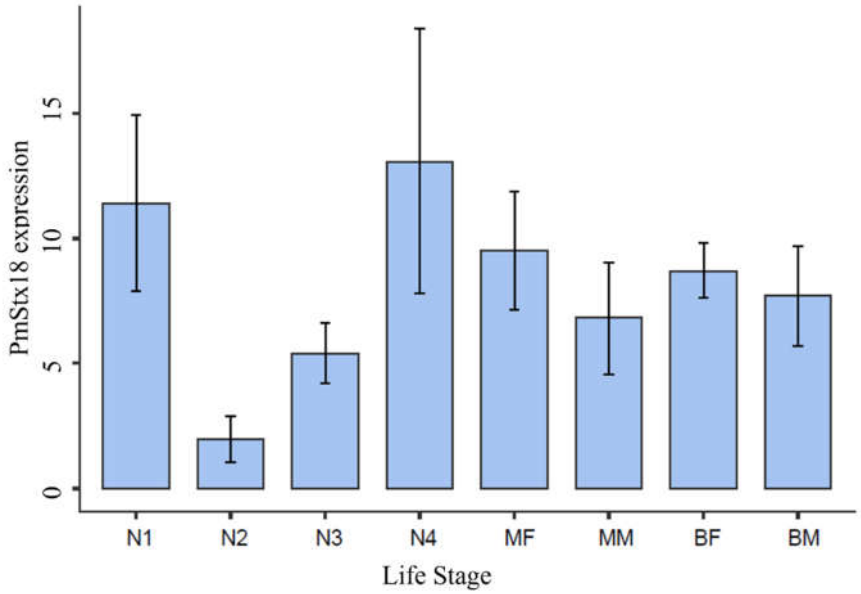

Figure 1. PmStx18 expression across *P. maidis* life stages: first nymphal stage (N1), second nymphal stage (N2), third nymphal stage (N3), fourth nymphal stage (N4), female macropter (MF), male macropter (MM), female brachypter (BF), male brachypter (BM). Expression was averaged across four trials. P= 0.043.

Alignment of the contig sequence with the original PmStx18 sequence where the primers were derived from resulted in 91.94% match, verifying that the gene amplified and analyzed in this study was indeed Syntaxin 18. The amplified sequence was 670 base pairs but spanned positions 64 to 800 of the original PmStx18 mRNA sequence. The two sequences differ in exactly 121 base pairs. It

 doi:10.20944/preprints202409.1580.v

included a six-nucleotide deletion and a 60-nucleotide deletion, the former at bases 301-307 and the latter spanning bases 519- 578. The rest of the 55 sequence variations were base substitutions. Discontiguous megablast and phylogenetic analysis of PmStx18 isolate showed high similarity and is clustering with its fellow delphacids and Hemipterans (Figure 2). The PmStx18 sequence obtained in this study (Genbank Accession OQ645740.1) enabled the design of dsRNA targeting PmStx18, which will be used to further investigate the function and role of Syntaxin 18 in *P. maidis* and in MMV infection, and to develop novel control methods such as RNA-mediated interference of PmStx18.

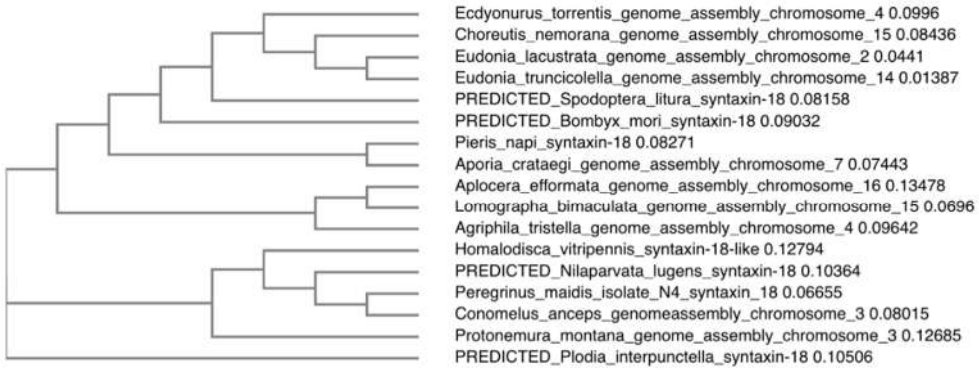

Figure 2. Phylogenetic analysis of representative hemipterans based on Stx18 sequences. *Peregrinus maidis* isolate N4 syntaxin 18 (Stx18) mRNA, partial cds GenBank: OQ645740.1 through discontiguous megablast.

The relatively high PmStx18 gene expression in the abdomen of female *P. maidis*, and on the head of male *P. maidis* is shown in Figure 3. Even though the bar plot shows that the head has a greater average expression, its relatively higher standard deviation can imply the variability of this data. Statistically, the expression of Stx18 in the major body parts are not significantly different (P= 0.228) in males and females. However, if we compare the expression of Stx18 between male and female, the latter significantly has higher expression compared to male (P= 0.037). This is similar to the result when whole insect samples were tested for Stx18 expression as mentioned above. In addition, Stx18 in abdomen of females have significantly higher expression compared to males (P= 0.0450). it can be determined that female *P. maidis* has a higher PmStx18 expression than male *P. maidis*. The higher PmStx18 gene expression in females may have been their mechanism of strengthening their cellular immune defense against possible infection for improved immunocompetency. Although having a longer lifespan than male *P. maidis*, females focus on enhancing their egg reproductivity due to environmental hindrances such as the presence of predators and fluctuating temperature. The higher expression of syntaxin 18 in females could have an underlying role in improving insect immunity. The Qa SNARE family has been revealed to have a role in enhancing the immune system of mammals. Syntaxin 11 has been found to be important in regulating the membrane dynamics of the immune system, suggesting its role in preventing pathogen assembly in thymus, spleen, and lymph nodes (Chen et al., 2015). In humans, syntaxin 18 has also been reported to influence the efficiency of phagocytosis, the process of engulfing pathogens (Nazario-Toole & Wu, 2017). Furthermore, a study by Barandoc-Alviar et al. (2016) revealed that the average MMV titer in male *P. maidis* is three-fold higher than female MMV titer, while, in the current study, the expression of PmStx18 is relatively higher in females than that of male. Thus, further demonstrating the role of syntaxin 18 in boosting the insect vector's immunity against MMV.

 doi:10.20944/preprints202409.1580.v

A.

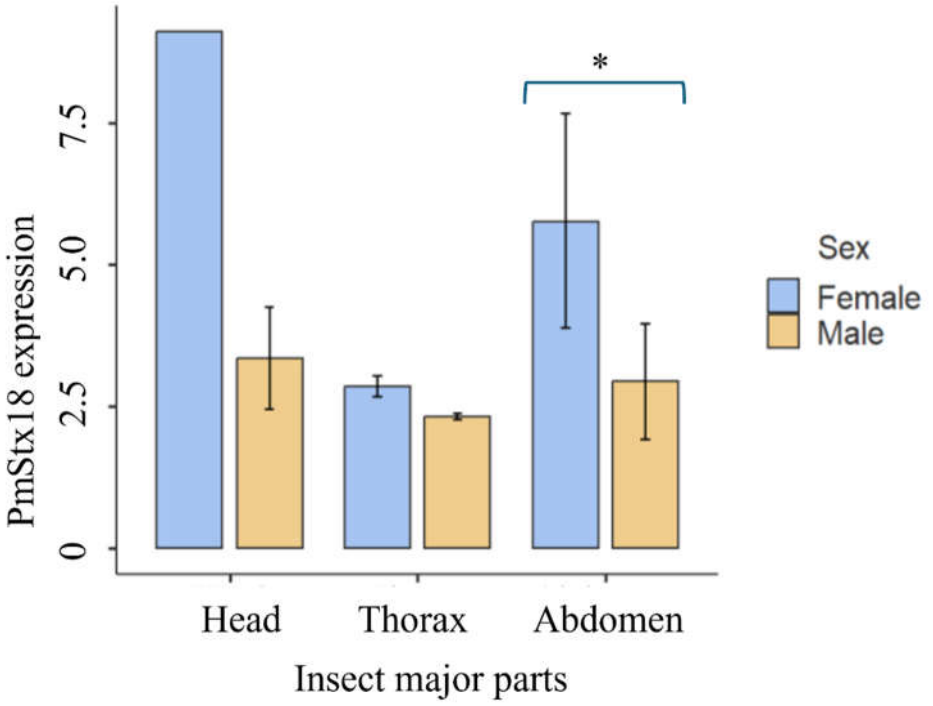

B.

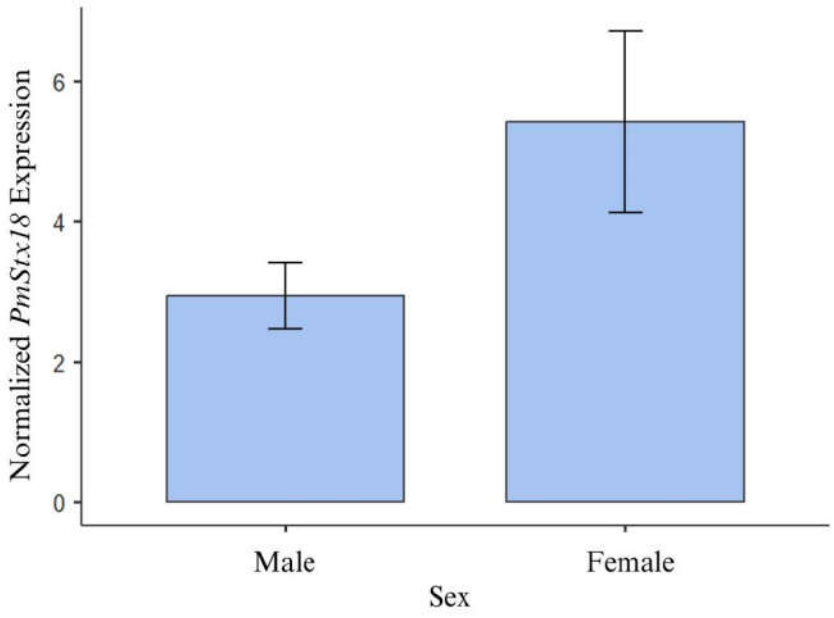

Figure 3. PmStx18 expression relative to RPL10. **A.** PmStx18 expression in the major insect parts, head, thorax and abdomen. Expression is averaged across four trials. P= 0.228. **B.** PmStx18 expression between male and female. Expression is averaged across four trials. P= 0.037.

While the functional role of *P. maidis* Syntaxin 18 in MMV infection has not been determined, Syntaxin 18 has been shown to colocalize with MMV-G (Barandoc-Alviar et al., 2022) and has shown strong predicted interactions in silico (Castrosanto et al., 2022) (Castrosanto et al., 2022). If this hypothesis holds, PmStx18 expression will be vital for the development of effective management strategies against *P. maidis* infestation and MMV transmission. RNA interference (RNAi) is a homology-directed, post-transcriptional mechanism of gene silencing triggered by double stranded RNA that has the potential to act as biopesticides targeting housekeeping genes or genes that play a major role in viral transmission. RNAi a post-transcriptional gene regulation mechanism that utilizes

 doi:10.20944/preprints202409.1580.v

short, double-stranded RNA molecules to silence specific genes (Fire et al., 1998). These RNA molecules can bind complementarily to messenger RNA (mRNA) molecules which either inhibits mRNA translation into proteins or triggers its degradation. This approach can be harnessed to selectively silence essential genes in insect vectors, potentially reducing virus transmission efficiency. This technology has been applied in the development of transgenic corn that expresses hairpin RNAs that target the Snf7 gene and *Bacillus thuringiensis* toxins against the western corn rootworm, *Diabrotica virgifera* virgifera (Head et al., 2017). The efficiency of RNAi, however, greatly depends on the developmental stage of the target insect and the amount of transcripts or gene expression of the target gene (Hoang et al., 2022). For any modern tool such as RNAi to be used to target Syntaxin 18 and successfully disrupt MMV transmission or *P. maidis* infestation, the developmental stage and gene expression would have to be considered for maximum efficiency. A recent study by Barandoc-Alviar et al. (2022) identified proteins in *P. maidis* that interacts with the MMV glycoprotein and this includes Syntaxin-18. This was further supported by evidence of the role of Syntaxin-18 in MMV proliferation within the insect vector. These findings highlight the potential of targeting Syntaxin-18 using RNAi technology as a novel strategy for controlling MMV infection**.** Previous experiment by Betz ((Betz & Kobs, n.d.)2003) elucidates the effect of dsRNA length for RNA interference in nonmammalian systems. His results show that shorter dsRNAs are as effective as longer dsRNAs. Thus, Fragment A was utilized for downstream experiments since it has the shortest fragment size and has the lowest penalty pair. Figure 4 demonstrates successful amplification of Fragment A using primers containing extended T7 promoter sequences. The amplified fragments exhibit the expected size of 400 base pairs and the prominent band of the diluted PCR product (2:5) indicates efficient amplification. Subsequently, this stipulates that the PCR cycling conditions is optimal.

A.

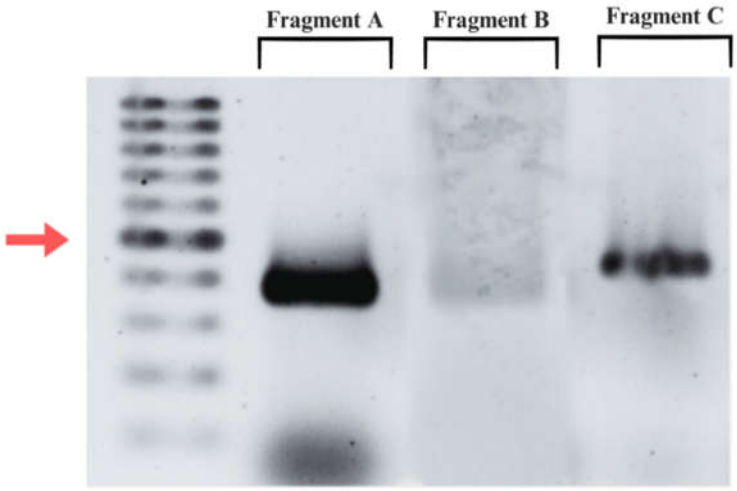

 doi:10.20944/preprints202409.1580.v

B.

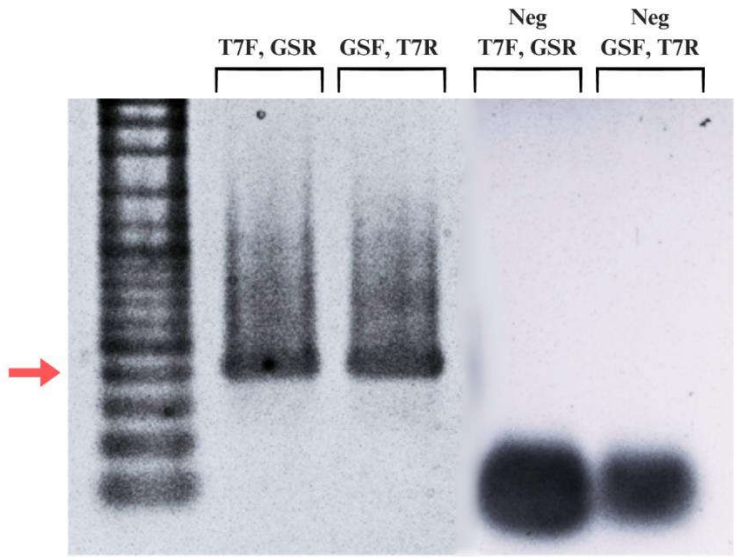

Figure 4. Amplification of designed dsRNA fragments targeting *P. maidis* Syntaxin-18 mRNA sequence. **A**. Agarose gel image of purified fragments A, B, C. **B**. PCR amplicon after attachment of extended T7 promoter sequences. Red arrow points to 400 bp.

Attaching promoter sequences to DNA fragments using PCR is a widely employed technique in molecular biology. However, this approach can present certain challenges. Design of the primer is crucial to ensure specific annealing to the target DNA while incorporating the desired promoter sequence. Long primer sequences are particularly prone to forming secondary structures or complementarily anneals with other primers to form dimers (Lorenz, 2012) where both scenarios significantly decrease PCR efficiency. PCR cycling conditions also require special consideration when working with extended primer sequences since mispriming may occur frequently (Lorenz, 2012). The four-stage PCR protocol addresses this concern by incorporating an initial cycle with stringent conditions to minimize mispriming and promote specific binding of the gene-specific region of the primer to the template (Lorenz, 2012). This strategy offers an advantage in generating the correct PCR product. After the initial 5-10 cycles, it is expected that there are numerous copies of the correct product over any amplicons produced by false priming. confirm the presence and integrity of the extended T7 promoter sequence incorporated using PCR amplification, the generated contigs were aligned with trimmed Fragment A sequence from the original *P. maidis* Syntaxin-18 mRNA sequence. As previously observed, there is a decrease in signal intensity towards the 3′ end during Sanger sequencing resulted in shorter contigs. Despite this, the alignment revealed successful attachment of the complete extended T7 promoter sequence to the sense strand of the DNA template. To visualize the dsRNA fragment produced, 5 µL of the diluted dsRNA (1:100) was loaded on to 1.5% agarose gel. Figure 5B shows the fragments generated from in vitro transcription of Fragment A and Green Fluorescent Protein (GFP). Double-stranded GFP is commonly used as a positive control in RNAi assays in several arthropod species (Nunes et al., 2013). The presence of band in the lane containing dsGFP implies that the reaction mix is functional and transcription successfully occurred. The expected size of the dsRNA fragment from Syntaxin-18 Fragment A is shorter than 374 bp (Figure 5C). Therefore, the target band is anticipated to migrate below the 374 bp marker on the gel. As observed in, a single faint band can be observed at approximately 200 bp which is consistent with the expected size. The Syntaxin-18 Fragment A (dsSTX18A) exhibited significantly high yield which translates to approximately 3.3 times the minimum expected yield. Considering the starting concentration of the DNA template, the increase of dsRNA concentration can be attributed to the high processivity of the T7 RNA polymerase. T7 RNA polymerase (T7RNAP) exhibits strong affinity for its promoter sequences which leads to efficient and rapid RNA synthesis (Borkotoky & Murali,

 doi:10.20944/preprints202409.1580.v

2018). Additionally, T7 RNA polymerase also exhibits high transcription rates which ranges from 50 to 90 nucleotides per second (Skinner et al., 2004). Lastly, the stable physiological conditions of the reaction and the absence of inhibitory substances likely contributed to the observed high yield (Table 2).

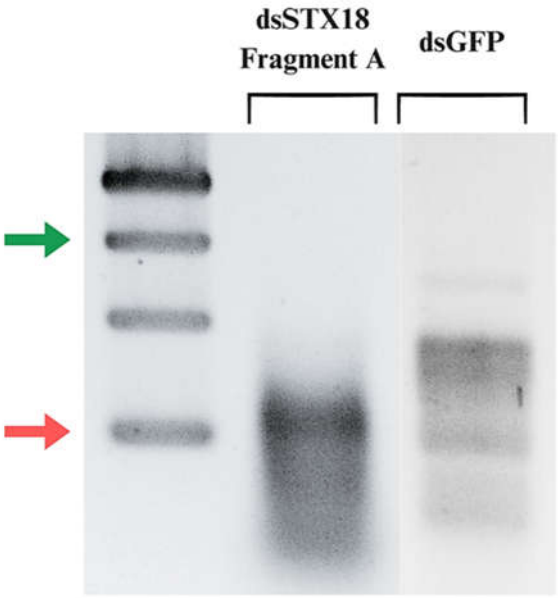

Figure 5. Agarose gel electrophoresis of dsRNA fragments generated from in vitro transcription of linearized PCR product templates of *P. maidis* Stx18 Fragment A and green fluorescent protein (GFP). The red arrow points to the 500 bp molecular marker, while the green one points to the 200 bp marker.

Table 2. Amount of dsRNA synthesized in ng/μL after in vitro transcription.

SAMPLE	A_{260}	DSRNA CONCENTRATION (NG/ML)	TOTAL AMOUNT OF DSRNA IN 40 ML (MG)	PERCENT YIELD (%)
dsSTX_A	0.072	57.33	229.00	
	0.093	73.90	296.00	
	0.081	65.09	260.00	
Average	0.082	65.44	262.00	327%

It is also important to note that the use of separate DNA templates for in vitro transcription is also crucial to the efficient production of dsRNA. Many studies employ another approach which utilizes a single DNA template containing the fragment of the target gene flanked by two convergent T7 RNA polymerase promoter sequences. This design allows for simultaneous transcription of both the sense and antisense mRNA in the same reaction mix, which can rapidly anneal to form dsRNA. However, one of the limitations of this method is unequal promoter activity which results to unequal concentration of the sense and antisense ssRNAs (Hough et al., 2022). The protocol used in this study addresses such limitation where two separate DNA templates are used. Each template contains a single T7 promoter sequence in its 5′ end of either the sense or antisense strand. Transcription occurs in separate reactions ensuring equal synthesis of both RNA strands. Thus, this results in high quality dsRNA suitable for downstream applications.

Summary and Recommendations

Further studies need to be conducted in order to validate the gene expression profile produced in this study. Better quantitative methods such are qRT-PCR, especially those comparing PmStx18

 doi:10.20944/preprints202409.1580.v

expression in MMV-infected and MMV-negative corn planthoppers would shed light on whether and how much the expression of the gene is affected by the virus. Several future studies are recommended to validate and optimize RNAi approach on silencing PmStx18 gene. First, cloning of the amplified fragments with T7 promoter sequences is recommended to prevent DNA template degradation by exonucleases. Plasmid vectors would provide a more stable and readily available DNA template for a more cost-effective dsRNA production. Second, bioassays are essential to evaluate the efficacy of the dsRNA fragments in silencing Syntaxin-18 expression within *P. maidis*. Monitoring changes in phenotypic characteristics of *P. maidis* would help elucidate the effects of PmStx18 silencing. It is also empirical to quantify the MMV titer within *P. maidis* following dsRNA treatment to determine the efficiency of RNAi approach to control MMV transmission. Lastly, quantification of the expression of Syntaxin-18 can also be done to confirm efficiency of gene silencing. These studies would ensure understanding of the effects of RNAi on the insect vector and determine the specificity of the approach for MMV control.

Acknowledgements: The authors wish to thank DA BIOTECH from the project with a fund code R1805 for their support to KBA leading to the purchase of her first PCR machine.

Conflict of Interest: The authors declare no conflict of interests in preparing this article for publication.

References

Alviar, K. B., Rotenberg, D., Martin, K. M., & Whitfield, A. E. (2022). The physical interactome between Peregrinus maidis proteins and the maize mosaic virus glycoprotein provides insights into the cellular biology of a rhabdovirus in the insect vector. *Virology*, *577*, 163–173.

Ammar, E.-D., Tsai, C.-W., Whitfield, A. E., Redinbaugh, M. G., & Hogenhout, S. A. (2009). *Cellular and molecular aspects of rhabdovirus interactions with insect and plant hosts*.

Barandoc-Alviar, K., Ramirez, G. M., Rotenberg, D., & Whitfield, A. E. (2016). Analysis of acquisition and titer of Maize mosaic rhabdovirus in its vector, Peregrinus maidis (Hemiptera: Delphacidae). *Journal of Insect Science*, *16*(1).

Barandoc-Alviar, K., Rotenberg, D., & Whitfield, A. (2015). Analysis of the virus-insect vector interactome of Maize mosaic rhabdovirus glycoprotein. *PHYTOPATHOLOGY*, *105*(11), 12.

Betz, N., & Kobs, G. (n.d.). *Optimal Generation of Short RNAs Using the T7 RiboMAX™ Express RNAi System*.

Castrosanto, M. A., Clemente, A. J. N., Whitfield, A. E., & Alviar, K. B. (2022). In silico analysis of the predicted protein-protein interaction of syntaxin-18, a putative receptor of Peregrinus maidis Ashmead (Hemiptera: Delphacidae) with Maize mosaic virus glycoprotein. *Journal of Biomolecular Structure and Dynamics*, 1–8.

Gorczyca, D., Ashley, J., Speese, S., Gherbesi, N., Thomas, U., Gundelfinger, E., Gramates, L. S., & Budnik, V. (2007). Postsynaptic membrane addition depends on the Discs-Large-interacting t-SNARE Gtaxin. *Journal of Neuroscience*, *27*(5), 1033–1044.

Hatsuzawa, K., Hirose, H., Tani, K., Yamamoto, A., Scheller, R. H., & Tagaya, M. (2000). Syntaxin 18, a SNAP receptor that functions in the endoplasmic reticulum, intermediate compartment, and cis-Golgi vesicle trafficking. *Journal of Biological Chemistry*, *275*(18), 13713–13720.

He, R., Zhang, J., Yu, Y., Jizi, L., Wang, W., & Li, M. (2018). New insights into interactions of presynaptic Calcium Channel subtypes and SNARE proteins in neurotransmitter release. *Frontiers in Molecular Neuroscience*, *11*, 213.

Hoang, B. T. L., Fletcher, S. J., Brosnan, C. A., Ghodke, A. B., Manzie, N., & Mitter, N. (2022). RNAi as a foliar spray: efficiency and challenges to field applications. *International Journal of Molecular Sciences*, *23*(12), 6639.

Lewis, M. J., Rayner, J. C., & Pelham, H. R. B. (1997). A novel SNARE complex implicated in vesicle fusion with the endoplasmic reticulum. *The EMBO Journal*.

Liu, C., Liu, D., Wang, S., Gan, L., Yang, X., & Ma, C. (2023). Identification of the SNARE complex that mediates the fusion of multivesicular bodies with the plasma membrane in exosome secretion. *Journal of Extracellular Vesicles*, *12*(9), 12356.

Lorenz, T. C. (2012). Polymerase chain reaction: basic protocol plus troubleshooting and optimization strategies. *JoVE (Journal of Visualized Experiments)*, *63*, e3998.

Napoli, C., Lemieux, C., & Jorgensen, R. (1990). Introduction of a chimeric chalcone synthase gene into petunia results in reversible co-suppression of homologous genes in trans. *The Plant Cell*, *2*(4), 279–289.

Patel, S. K., Indig, F. E., Olivieri, N., Levine, N. D., & Latterich, M. (1998). Organelle membrane fusion: a novel function for the syntaxin homolog Ufe1p in ER membrane fusion. *Cell*, *92*(5), 611–620.

Roberts, A. F., Devos, Y., Lemgo, G. N. Y., & Zhou, X. (2015). Biosafety research for non-target organism risk assessment of RNAi-based GE plants. *Frontiers in Plant Science*, *6*, 958.

Schmittgen, T. D., Zakrajsek, B. A., Mills, A. G., Gorn, V., Singer, M. J., & Reed, M. W. (2000). Quantitative Reverse Transcription–Polymerase Chain Reaction to Study mRNA Decay: Comparison of Endpoint and Real-Time Methods. *Analytical Biochemistry*, *285*(2), 194–204. https://doi.org/https://doi.org/10.1006/abio.2000.4753